

Supporting Information

Porous Graphdiyne Applied for Sodium Ion Storage

*Shengliang Zhang,^{a,b,‡} Jianjiang He,^{a,b,‡} Jie Zheng,^{a,b,‡} Changshui Huang,^{*a} Qing Lv,^a*

*Kun Wang,^a Ning Wang,^a and Zhenggang Lan^{*a}*

^a Qingdao Institute of Bioenergy and Bioprocess Technology, Chinese Academy of Sciences, No. 189 Songling Road, 266101, Qingdao, China.

^b University of Chinese Academy of Sciences, No. 19A Yuquan Road, 100049, Beijing, China.

[‡] These authors contributed equally

^{*} Corresponding author.

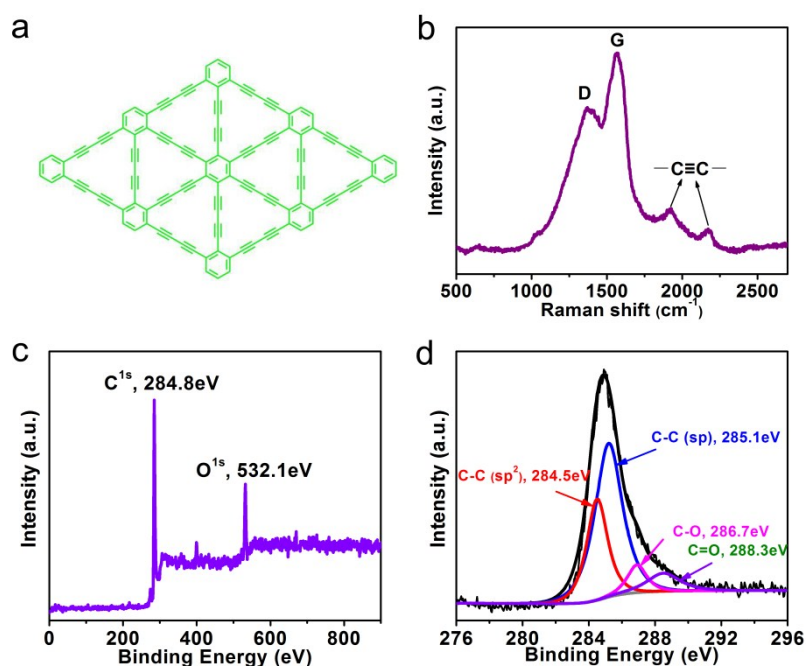


Fig. S1 (a) The structural representation of a GDY sheet, (b) Typical Raman spectrum of GDY, (c) Survey and (d) C 1s binding energy profiles of GDY.

Raman spectra of bulk GDY (Figure S1b) exhibits two prominent peaks at about 1367.4 cm^{-1} and 1567.5 cm^{-1} , corresponding to the typical D band and G band for carbon materials. The intensity of the D band is strongly associated with structural defects, including disordered carbon atoms and edges; the G band corresponds to first-order scattering of the E_{2g} stretching vibration mode observed for sp^2 -hybridized carbon atom domains in aromatic rings. Generally, the intensity ratio of D band and G band (I_D/I_G) is used to estimate the disorder and defects of GDY. The I_D/I_G of GDY was 0.71, suggesting bulk GDY powders possess high order and low content of defects. The peaks at 1921.1 and 2171.8 cm^{-1} were contributed by the vibration of acetylenic linkages ($-\text{C}\equiv\text{C}-\text{C}\equiv\text{C}-$). As shown in Figure S1c, the survey scan spectra displayed a pronounced XPS C 1s peak at 284.8 eV, and a weaker O 1s peak at 531.6 eV. The presence of a signal for O 1s arose from the adsorption of O_2 when GDY was exposed to air. After subtraction of the Shirley background, followed by fitting with a mixture function of Lorentzian and Gaussian, the C 1s peak (Figure S1d) could be divided into four mainly sub-peaks at 284.5, 285.1, 286.7, and 288.3 eV, which could be assigned to orbitals in C-C (sp^2), C≡C (sp), C-O, and C=O bonds, respectively. The area ratio of the sp - and sp^2 -hybridized carbon atoms was 2, which confirmed the structure of GDY comprising benzene rings linked together through two acetylenic linkages.

Table S1. Overview of different types of carbon as anodes for sodium ion batteries.

Type of Carbon	Potential Range (V vs Na ⁺ /Na)	Current Densities (mA g ⁻¹)	Capacities (mAh g ⁻¹)	Surface Area (m ² g ⁻¹)	Additional Information	Citation
Hard carbon	0-3	30	290		100 cycles with 93% of capacity retention	10
Hollow carbon nanospheres	0-3	50	223	410	at 50 mA g ⁻¹ for first 10 cycles and then 100 mA g ⁻¹ for next 100 cycles, a reversible capacity of 160 mAh g ⁻¹ is stably obtained.	11
Hollow carbon nanowires	0.01-1.2	50	251	34.1	82.2% capacity retention over 400 cycles at 50 mA g ⁻¹ , a reversible capacity of 149 mAh g ⁻¹ at 500 mA g ⁻¹ .	12
N-doped porous carbon fibres	0-3	50	296	372.4	a reversible capacity of 72 mA h g ⁻¹ at 10 A g ⁻¹	13
Graphite	-0.5-2	37.2	close to 100		1000 cycles with coulombic efficiencies > 99.87%	15
Expanded graphite	0-2	20	284		maintain a capacity of 184 mAh g ⁻¹ at 100 mA g ⁻¹ , retain 73.92% of its capacity after 2000 cycles	17
Reduced grapheme oxide	0.01-2	40	174.3	330.9	a high capacity of 141 mAh g ⁻¹ at 40 mA g ⁻¹ over 1000 cycles	18
Carbon black	0-1.5	4.96	~130	22.1		
Porous graphdiyne	0.005-3	50		287.7	a reversible of capacity of 261 mAh g ⁻¹ after 300 cycles at 50 mA g ⁻¹ , an excellent capacity retention of 98.2 % after 1000 cycles at 100 mA g ⁻¹	This work

The citations in this Table are related to the references in the main article.

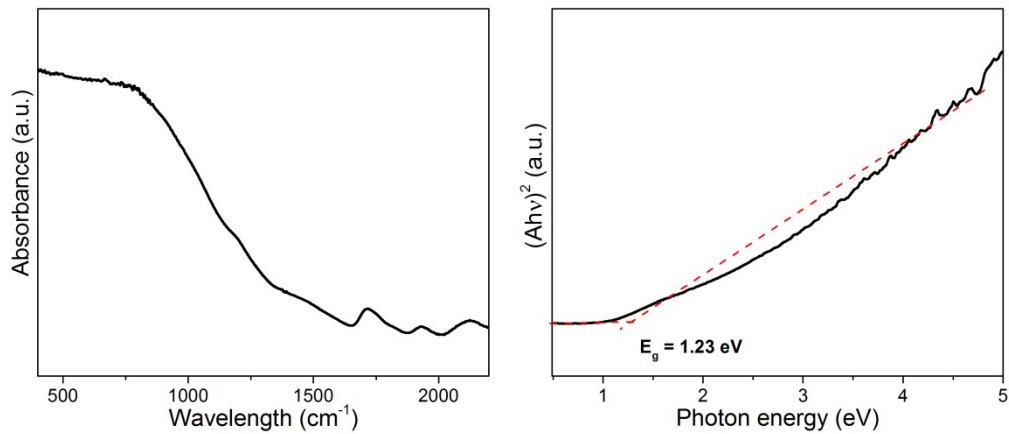


Fig. S2 UV-Vis spectrum of porous GDY. And plots of $(Ah\nu)^2$ versus photon energy ($h\nu$).

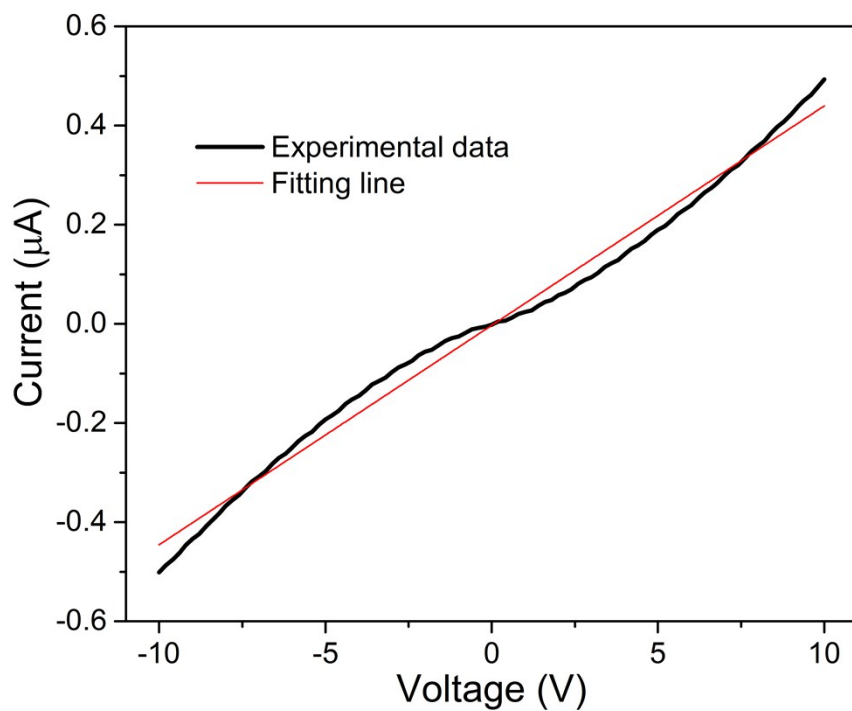


Fig. S3 I-V curve of porous GDY.

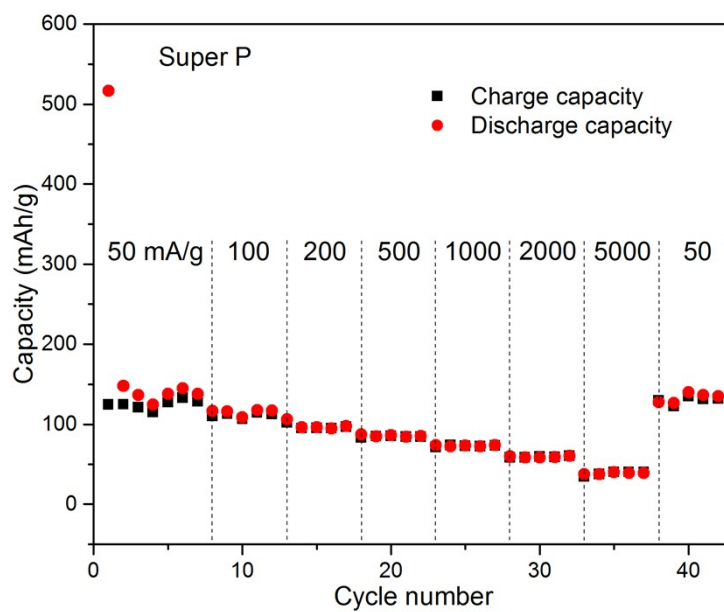


Fig. S4 Rate performance of super P in a sodium half-cell.

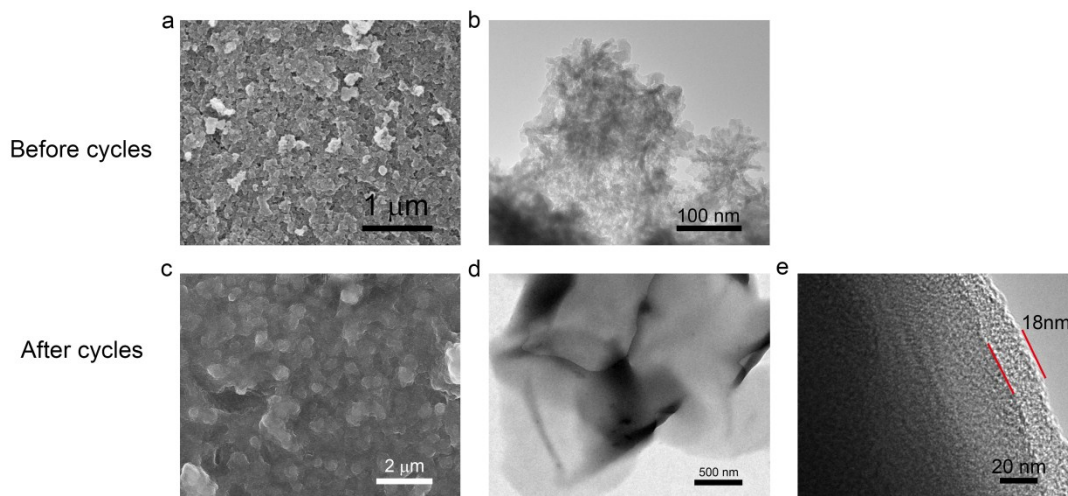


Fig. S5 (a, c) SEM images and (b, d and e) TEM images of porous GDY before and after cycles.

References

- 10 J. Zhao, L. Zhao, K. Chihara, S. Okada, J.-i. Yamaki, S. Matsumoto, S. Kuze and K. Nakane, *J. Power Sources*, 2013, 244, 752.
- 11 K. Tang, L. Fu, R. J. White, L. Yu, M.-M. Titirici, M. Antonietti and J. Maier, *Adv. Energy Mater.*, 2012, 2, 873.
- 12 Y. Cao, L. Xiao, M. L. Sushko, W. Wang, B. Schwenzer, J. Xiao, Z. Nie, L. V. Saraf, Z. Yang and J. Liu, *Nano Lett.*, 2012, 12, 3783.
- 13 L. Fu, K. Tang, K. Song, P. A. van Aken, Y. Yu and J. Maier, *Nanoscale*, 2014, 6, 1384.
- 15 B. Jache and P. Adelhelm, *Angew. Chem. Int. Ed.*, 2014, 53, 10169.
- 17 Y. Wen, K. He, Y. Zhu, F. Han, Y. Xu, I. Matsuda, Y. Ishii, J. Cumings and C. Wang, *Nat. Commun.*, 2014, 5, 4033.
- 18 Y.-X. Wang, S.-L. Chou, H.-K. Liu and S.-X. Dou, *Carbon*, 2013, 57, 202.